Insights on the Interactions of Chitosan with Phospholipid Vesicles. Part II: Membrane Stiffening and Pore Formation

Omar Mertins*,† and Rumiana Dimova*

Department of Theory and Bio-Systems, Max Planck Institute of Colloids and Interfaces, Science Park Golm, 14424 Potsdam, Germany

Ⓢ *Supporting Information*

ABSTRACT: The interactions between the polysaccharide chitosan and phospholipids are studied using giant unilamellar vesicles (GUVs). We explore both bare GUVs incubated in chitosan solution post vesicle formation and GUVs prepared using a reverse-phase method where the polymer is adsorbed on both sides of the membrane leaflet. The fluctuations of the vesicle membrane are significantly reduced in the presence of chitosan as characterized by the bending rigidity, which increases with chitosan concentration denoting physical restrictions imposed to the bilayer as a consequence of the interaction with the polysaccharide. In the absence of chitosan, the rigidity of the bare phosphatidylcholine vesicles is also observed to increase (about 3-fold) upon the incorporation of a small fraction (10 mol %) of phosphatidylglycerol. Pore formation caused by chitosan is evidenced by loss of optical contrast of the giant vesicles denoting exchange between internal and external solutions through the pores. Our study provides evidence for the potential of chitosan to affect the bilayer permeability and to disrupt negatively charged membranes as well as to promote adhesiveness of vesicles on glass surfaces.
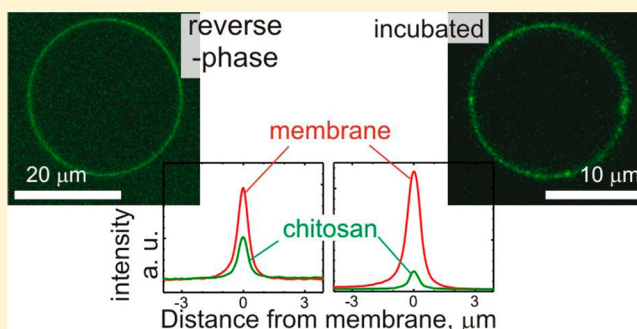
1. INTRODUCTION

The polysaccharide chitosan is regarded as a macromolecule with interesting advantages in the development of a variety of materials intended for biomedical applications.[1−6] Specifically, in the field of drug delivery, nanoparticles and formulations containing chitosan have shown promising results in the search of drug release systems optimizing disease treatments and with reduced drug side effects.[7−10] The amino groups of the polymer monomers grant to chitosan relatively good solubility in aqueous solutions as well as ensure electrostatic interactions with phospholipids that build cell (bacterial) membranes.[11] These properties have been employed in the development of composite phospholipid-chitosan vesicles as new structures for encapsulation of drugs and vaccines aimed as vectors and tolls for controlled antigen release.[12−16] However, the specificity of the application sites requires detailed knowledge of the particular structures.

In recent years, the physicochemical features of the interaction of chitosan with liposomes have been a target of scrutiny.[17,18] The polysaccharide influences the structural characteristics of submicrometric vesicles, alters the repeat distance in bilayer stacks as well as the thermal stability of phospholipid membranes.[19,20] As a soft matter, the vesicle membrane may endure remarkable disturbances in the presence of the polysaccharide. A way to visualize the direct response of the membrane upon the encounter with chitosan is provided by means of employing giant unilamellar vesicles (GUVs).[21,22]

In the present Article, we describe further attempts to elucidate physical parameters characterizing the chitosan–membrane system and explore the effect of the polymer on the membrane mechanical properties. Two main approaches of preparing giant vesicles coated with chitosan (giant chitosomes) have been previously reported. One is based on simply incubating the preformed lipid vesicles in chitosan solutions,[23] whereby only the external leaflet of the membrane is immediately accessible to the adsorbing polymer. The second approach employs electroformation procedure for GUV formation based on a reverse-phase precursor.[24] In this production methodology, chitosan is strongly interacting and covering both sides of the phospholipid bilayer and consequently is expected to alter the membrane stiffness significantly. We determine the membrane bending rigidity via fluctuation analysis of giant vesicles prepared by both ways.

It is known that the strong interaction of chitosan with phospholipids may influence the membrane permeability and make negatively charged membranes leaky.[25−27] For the model giant vesicles, we show that chitosan adsorption can lead to pore formation, permeability increase, disruption and morphological changes in the vesicles. The adhesive property of the polymer is also evidenced by strong adhesion and rupture of chitosan-coated vesicles onto glass surfaces.

2. EXPERIMENTAL SECTION

2.1. Materials. Chloroform solution of 1,2-dioleoyl-*sn*-glycero-3-phosphatidylcholine (DOPC), 1,2-dioleoyl-*sn*-glycero-3-phosphatidyl-glycerol (sodium salt) (DOPG), and fluorescent dipalmitoylphospha-tidylethanolamine-*N*-lissamine rhodamine B sulfonyl (DPPE-Rhod) were purchased from Avanti Polar Lipids Inc. (Birmingham, AL) and used without further purification. They were stored at −20 °C upon arrival. Chitosan was a gift from Primex (Germany), with 95% degree of deacetilation (DDA). The average molecular weight was determined as M_w = 199 kDa (corresponding to 1223 repeat monomers per molecule) by multiangle laser light scattering size exclusion chromatography (MALLS-SEC),[28] with a radius of gyration of 46 nm.

Fluorescent chitosan was obtained as previously described,[24] introducing the fluorescent probe FITC (fluorescein isothiocyanate isomer I; 90%; Fluka BioChemika) on few polymer monomers in a proportion of 1:100 (labeled to not labeled monomers) according to the procedure of Qaqish and Amiji.[29] Fluorescent chitosan was used only for confocal microscopy measurements with giant vesicles.

All other reagents were of analytical grade. All solutions were prepared using deionized water from Milli-Q Millipore system with a total organic carbon value of less than 15 ppb and a resistivity of 18 MΩcm.

2.2. Preparation of Chitosan Solutions. The chitosan solution was prepared by vigorous overnight stirring of the powder in aqueous acetate buffer solution of acetic acid/sodium acetate (80 mM, pH 4.48 ± 0.01), at a concentration of 1 mg/mL. Solutions with lower concentrations were prepared by diluting the stock solution with buffer. The pH of all solutions was constantly monitored before and after sample preparation, and the conductivity was measured, to ensure constant ionic strength. Acetic acid was added to adjust the pH when required.

2.3. Preparation of Bare Giant Vesicles and Incubation with Chitosan. Lipid stock solution in chloroform (10−20 µL, 1 mg/mL) was spread on two conductive glass substrates coated with indium tin oxide (ITO). The lipid films were dried in a vacuum desiccator for at least 2 h. A rectangular Teflon frame of thickness 1.6 mm served as a chamber spacer between the two opposing glass substrates. The chamber was sealed with silicone grease. The coated ITO surfaces acted as electrodes. Approximately 2 mL of sucrose solution at concentration of 10 mM was introduced into the chamber through a 0.22 µm sterile filter (Millipore). Alternating electric field of 1.5 V (peak-to-peak) and 10 Hz was immediately applied using a function generator (Agilent 33220A 20 MHz function/arbitrary waveform generator). The field was applied for 1−2 h, after which the vesicle suspension was carefully transferred to an Eppendorf vial.

Vesicles were prepared from pure DOPC or a mixture of DOPC and DOPG (90 and 10 mol %). Fluorescently labeled vesicles were prepared using 0.1 mol % of DPPE-Rhod added to the lipid stock solutions. Giant vesicles made of DOPC containing chitosan on the external leaflet of the membrane were prepared by incubation in an Eppendorf vial. 700 µL of the vesicle solution was mixed with 20 µL of chitosan solution (0.100 mg/mL) containing the appropriate amount of sucrose to obtain the same osmolarity as that of the original vesicle solution in order to avoid osmotic shocks. The osmolarities of all solutions were measured and adjusted using osmometer Osmomat 030 (Gonotec, Germany). The incubation was done during one hour right before the microscopy observations and measurements. The resultant pH of chitosan incubated vesicles solution was the same as that of the chitosan buffer solution, that is, close to 4.5. At these conditions, the polymer is highly protonated, exhibits no self-aggregation and interacts relatively weakly with DOPC/DOPG membranes.[30] Before microscopy observations, the giant chitosomes (50 µL) were further diluted in an isotonic glucose solution (200 µL). Due to the lower density of the glucose solution, the vesicles sediment to the bottom of the observation chamber. The final pH of the solution was slightly higher (around 4.7) enhancing the interaction of the polymer with the charged membrane.

2.4. Preparation of Reverse-Phase Giant Vesicles. Giant vesicles containing chitosan on both sides of the phospholipids bilayer were prepared according to the method of Mertins et al.[24] Differently from the usual electroformation procedure, instead of a solution of lipids in organic solvent, a reverse-phase emulsion of lipids and chitosan was spread over the ITO glasses. The emulsion was prepared by sonicating the mixture of lipids in chloroform and the appropriate amount of chitosan aqueous solution.[24] Typically, 200 µL of lipid solution at concentration of 1 mg/mL was mixed with 5−20 µL of chitosan aqueous solution at concentration of 1 mg/mL. After spreading part of the emulsion (20 µL) over the ITO glasses, the usual steps in the electroformation protocol as described above were followed. This method has proved efficient in increasing the interactions between phospholipids and chitosan and thus yields good-quality composite giant vesicles. Finally, 50 µL of the GUVs solution was dispersed in 200 µL of an isotonic glucose solution. The final pH of the solution was around 5.8.

2.5. Fluctuation Analysis on GUVs. A typical observation experiment, using an inverted optical microscope (see below), was made in an observation chamber, made of two microscope glass slides separated by 1 mm-thick press-to-seal silicone isolator (Molecular Probes). The slight density difference between the inner and outer solutions drove the vesicles to the bottom slide of the chamber where they could easily be observed. The concentration of the glucose solution used to dilute the vesicles was chosen a little bit higher than that of sucrose resulting in slightly deflated vesicles in the solution.

We used an inverted microscope Axiovert 135 (Zeiss, Germany) equipped with 20× and 40× objectives to visualize the GUVs under phase contrast mode. Image sequences were recorded with a fast digital camera HG-100K (Redlake Inc., San Diego, CA) and stored in the on-board memory of the camera head (total of 4 GB), and afterward downloaded to the computer. The images were analyzed to detect the vesicle contours over time, followed by analysis of the fluctuations as reported in detail previously.[31] The vesicle images were recorded for over 1 min with exposure time of 180 µs and acquisition rate of 125 frames per second. A mercury lamp HBO W/2 was used to acquire images of fluctuating vesicles using the fast digital camera. All experiments were performed at room temperature (23 ± 0.5 °C).

2.6. Confocal Microscopy. Samples of fluorescently labeled vesicles were transferred in the observation chamber, which was precoated as described in section 2.7. The vesicles were observed with a confocal microscope (Leica TCS SP5) with 63× water immersion objective. The fluorescent dyes where excited with a diode-pumped solid-state laser at 540 and 470 nm and the emission signal was collected around 625 and 525 nm for DPPE-Rhod and fluorescent chitosan (FITC-labeled) respectively.

2.7. Coating of Microscopy Glass Slides with Albumin. Thin glass slides used to build the chamber for observation of giant vesicles under the microscope were precoated with bovine serum albumin (BSA; Sigma) to avoid adhesion of chitosan containing vesicles. The glass slides were vigorously washed sequentially with water, ethanol, acetone, and chloroform and dried under nitrogen stream. The slides were then immediately immersed in the BSA aqueous solution (1 mg/mL) and incubated for 30 min. Afterward, the slides were dried under nitrogen and immersed in glucose solution (the same used for vesicle preparation) for 10 min. The slides were dried again and the two immersion steps were repeated three times before assembling the slides.

3. RESULTS AND DISCUSSION

3.1. Preparation of Giant Chitosomes. We present results for mainly six different kinds of vesicles: (1) bare vesicles made of 100% DOPC; (2) bare vesicles made of DOPC/DOPG 90/10 (molar fractions); (3) 100% DOPC giant vesicles prepared by the reverse-phase method using three different surface concentrations of chitosan, as previously studied in ref 24; (4) 100% DOPC vesicles incubated with 0.100 mg/mL chitosan after preparation. Other compositions and conditions were also explored as described in the following and listed in Table S1 in the Supporting Information.

Bare giant vesicles made of DOPC/DOPG 90/10 were easier to prepare than pure DOPC vesicles. With the presence of the negatively charged phospholipid, the vesicles grow faster under the same electroformation conditions (see Experimental Section) and they can even be formed spontaneously.[32] However, difficulties arise when electroforming chitosan-coated DOPC/DOPG vesicles using the reverse-phase method. The vesicles were too small, aggregated and with many buds, which is why we were not able to explore their mechanical properties as discussed in the next section. This behavior might imply instability of the lamellar phase in the presence of chitosan. Giant DOPC/DOPG vesicles incubated with chitosan after formation appeared to be unstable as we will discuss in more detail further below. Pure DOPC vesicles incubated in chitosan solutions of high concentration were also unstable. This limitation, as well as the aim to match the chitosan coverage of incubated and reverse-phase vesicles, set the ranges of explored polymer concentrations.

Since we were not able to directly measure the concentration of adsorbed polymer in the case of the incubated vesicles, we roughly estimated the upper limit of chitosan monomers per lipid. We assumed that there is no lipid loss during the vesicle preparation, mixing and transfer in the observation chamber, and that only the outer leaflet of the vesicle membrane is accessible for binding. The upper limit for the surface concentration of the polymer estimated in this way is 4.15 chitosan monomers per lipid. Adsorption isotherms conducted in previous studies[33] indicate that for pure DOPC vesicles at these conditions, the amount of adsorbed polysaccharide corresponds to 0.10−0.35 monomers per accessible lipid. Isothermal titration calorimetry data for this range of chitosan-to-lipid ratios (and in general above ratios of chitosan monomers to accessible lipid around 0.1) suggest that the membrane surface of the DOPC/DOPG incubated vesicles is well saturated by the adsorbed chitosan; see Figure 3A in the accompanying work.[30]

To gain more insight about the distribution of the polymer over the membrane, we examined the giant chitosomes (prepared with both methods) with confocal microscopy using chitosan labeled with fluorescein and a small fraction of fluorescent lipid (0.1 mol % DPPE-Rhod). The two dyes emit in different wavelength ranges and thus the adsorbed chitosan can be distinguished from the labeled membrane. For vesicles prepared with the reverse-phase method, we observe colocalization of the fluorescent signal from the lipid and the labeled chitosan (see Figure S1 in the Supporting Information), as previously described.[24] Similarly, pure DOPC vesicles incubated with chitosan exhibit rough colocalization of the fluorescent signal from the lipid and the labeled chitosan as reported in reference.[34] However, chitosan appears to be inhomogeneously distributed over the membrane of the incubated vesicles compared to the reverse-phase vesicles as shown in Figure 1A, B. The incubated vesicles exhibit many highly fluorescent spots on the membrane alternating with segments of lower fluorescence. The inhomogeneous distribution of chitosan over the membrane is more clearly perceivable from the angular dependence of the fluorescence intensity along the vesicle contour; see Figure 1C, D (the intensity analyses were performed following the procedure outlined in ref 35; see also the Supporting Information for details). Presumably, the polymer has clustered or folded on the membrane producing spikes of fluorescence. We cannot
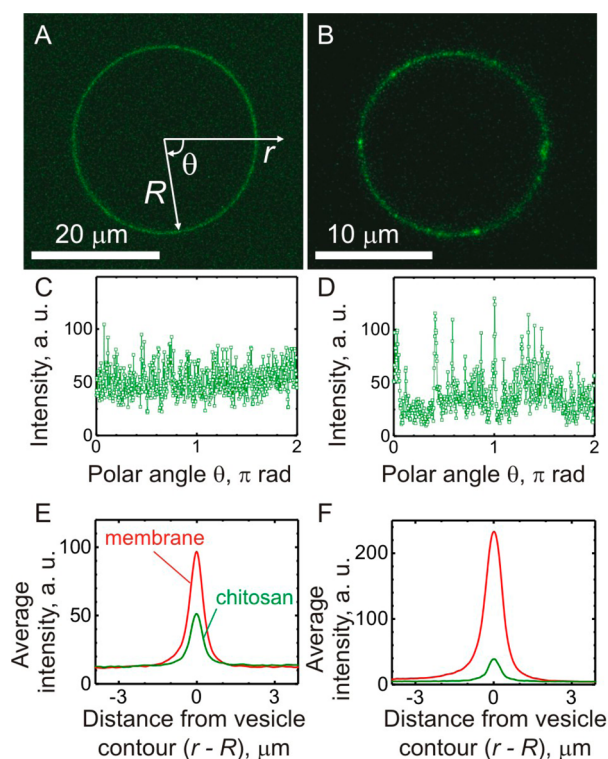
Figure 1. Confocal microscopy images of giant DOPC chitosomes with fluorescently labeled chitosan (green false color) and intensity analysis. Chitosan is more homogeneously distributed on the vesicle prepared with the reverse-phase method (A, C) where the polymer is present on both membrane leaflets, compared to the vesicle incubated in chitosan (B, D), where the polymer adsorbs only to the external membrane leaflet. The incubation was done in 0.100 mg/mL solution of chitosan (corresponding to 1.39×10^{-8} M monomeric chitosan) yielding an upper limit of 4.15:1 for the ratio of total chitosan monomers to accessible lipids. The ratio of adsorbed monomeric chitosan to accessible lipids for the reverse-phase vesicle was 8.1:100 (see text for detail). The angular dependencies of the intensity along the vesicle membrane for the vesicles in (A) and (B) are shown in (C) and (D), respectively; the polar angle θ as well as the vesicle radius R and the radial coordinate r are sketched in (A). The large scatter in the intensity for the incubated vesicles (D) shows strong inhomogeneity of the membrane coverage by chitosan. The radial dependencies of the intensity averaged over the polar angle for the membrane dye (red) and chitosan (green) for the reverse-phase and the incubated vesicles are given in (E) and (F), respectively.

exclude that in these regions the lipid bilayer has also folded on itself held together (or bridged) by the polymer.

Apart from the inhomogeneous chitosan adsorption over the membrane of the incubated vesicles, we also observe uneven distribution of the polymer over different vesicles in the same sample. Figure 2 shows two incubated DOPC vesicles clearly detected from the DPPE-Rhod fluorescence (Figure 2A). However, chitosan fluorescence is detected mainly on one of the vesicles while the emission from the other is almost imperceptible (Figure 2B). Hence, with the incubation protocol for giant chitosome formation, a larger amount of chitosan may incorporate in the membrane of some vesicles, while others remain with lower coverage. The vesicle in Figure 1B is an example for the former. Presumably, the observed inhomogeneity arises because the adsorption process is faster than the complete mixing of the solutions in the chamber. No stirring
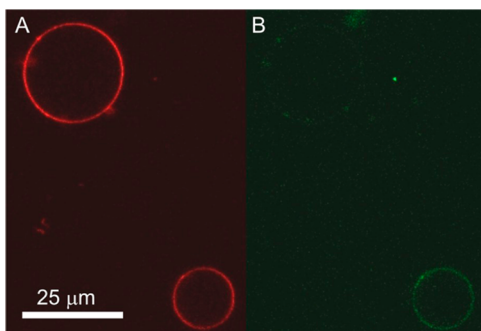
Figure 2. Confocal microscopy cross section of two incubated DOPC vesicles showing the uneven distribution of chitosan over different vesicles in the sample. The red signal shows fluorescence from the membrane (A), while the green signal is fluorescence from the labeled chitosan (B). The vesicle in the lower right corner of the images is covered with more chitosan compared to the larger vesicle in the upper left corner. The vesicles were incubated in 0.100 mg/mL solution of chitosan (corresponding to 1.39×10^{-8} M monomeric chitosan); after dilution in glucose, the final concentration of chitosan was 6×10^{-4} mg/mL.

was applied to avoid mechanical rupture of the GUVs. Thus, mixing occurred mostly under convection and diffusion.

Even when considering only the vesicles with denser coverage, overall, we detect lower signal from chitosan on the incubated vesicles compared to the reverse-phase vesicles. On the two vesicle types, we measured the radial distribution of the fluorescence signal of both the polymer and the membrane dye and averaged it over the polar angle; see the green and red curves, respectively, in Figure 1E, F. The ratio of the integrated chitosan intensity (green curves in Figure 1E, F) to the integrated membrane intensity (red curves) is a quantitative measure for comparing the amount of adsorbed polymer on the two vesicle types; see the Supporting Information. For the reverse-phase vesicle in Figure 1, this ratio is around four times larger compared to the ratio measured on the incubated vesicle. Note that the latter vesicle is representative for a well-coated vesicle; others in the same sample exhibit less chitosan fluorescence. We conclude that the amount of adsorbed polymer on the reverse-phase vesicles is at least 4-fold higher than that on vesicles incubated in chitosan solutions. This outcome is surprising, considering that the proportion of chitosan monomers to lipids according to adsorption isotherms[33] for the incubated vesicles (0.10−0.35) is high compared to that for the reverse-phase vesicles (0.081). However, we see that the incubated ones exhibit much weaker fluorescence (note that the polymer distribution is uneven both

over the membrane and between different vesicles in the sample). One reason for the lower amount of polymer adsorbed on the incubated vesicles is that mainly the external leaflet of the membrane is accessible for binding (no chitosan on the interior of the vesicles). Yet another reason could be the stronger physical interaction of chitosan with the lipids ensured in the case of the reverse-phase approach.

3.2. Morphology and Mechanical Properties of Giant Chitosomes. In this section, we first consider the effect of chitosan on the membrane mechanical properties of the vesicles. The bending rigidity of the bare vesicles and the chitosomes was measured by fluctuation analyses (or flicker spectroscopy) using an approach described previously.[31] The method consists of collecting sequential images of a fluctuating vesicle, detecting the contour of the vesicle on each image, and carrying out statistical analysis of the modal distribution, from which the bending rigidity is extracted.[31] The values for the bending rigidity κ obtained for the different vesicle types explored here are given in Table 1.

The data obtained for the chitosan-free pure DOPC vesicles is in very good agreement with data reported in the literature.[31,36,37] We are not aware of reports on the bending rigidity of charged DOPC/DOPG membranes. Our results (Table 1) show that the bending rigidity of DOPC vesicles increases around 3-fold upon the addition of 10% DOPG in the membrane. This increase in κ could be expected considering that charged phospholipids have increased polar head repulsion, which effectively suppresses the membrane undulations and thus increases the membrane rigidity as theoretically predicted.[38] Furthermore, the presence of the electric double layer surrounding a charged membrane is expected to increase the bending rigidity as theoretically predicted,[38−40] and experimentally confirmed on mixtures of phosphatidylcholine with phosphatidylserine[41,42] or ionic surfactants.[43] The presence of the surface charge, whether from the charged lipids or from the adsorbed chitosan (as we will see below), leads to stiffening of the membrane.

Similar increase in the bending rigidity was found for reverse-phase DOPC vesicles containing the smaller amount of chitosan; see Table 1. Following an approach outlined in ref 24, the amount of chitosan on the membrane of these vesicles was estimated to be 8.1 chitosan monomers for every 100 DOPC molecules considering both leaflets of the vesicle membrane, or equivalently 0.03 mg of chitosan/1 m² of DOPC. Apparently, this small amount of adsorbed chitosan is sufficient to significantly suppress the bilayer undulations increasing the bending rigidity of the membrane to an extent to which the addition of 10 mol % DOPG does.

Table 1. Bending Rigidity, κ, of Membranes with Various Compositions As Obtained by Fluctuation Analyses Performed at 23 $\pm$ 0.5 °C[a]

			vesicles with chitosan (Ch)				
	bare (chitosan-free) vesicles		vesicles prepared via the reverse-phase method[b]			vesicles incubated in 0.100 mg/mL chitosan after electroformation[c]	
	DOPC	DOPC/DOPG (90/10)	DOPC:Ch (100:8.1)	DOPC:Ch (100:13.5)	DOPC:Ch (100:27.1)	DOPC:incCh	DOPC/DOPG (90/10) :incCh
κ (10^{-20} J)	12.5 ± 3.2	36.1 ± 5.3	34.7 ± 5.8	42.4 ± 6.1	no fluctuations	62.9 ± 23.8	(≥49) vesicles collapse

[a]The error in κ represents standard deviation from the mean value for a population of at least 12 vesicles. [b]The proportion between DOPC and bound chitosan (DOPC:Ch) is represented as number of chitosan monomers for every 100 DOPC molecules and calculated from ref 24 where the same reverse-phase method for vesicle preparation was used. [c]For the vesicles incubated with chitosan (incCh), the polymer content on the membrane is unknown but on the order of 10−35 chitosan monomers per 100 lipids in the outer leaflet; see text for details.
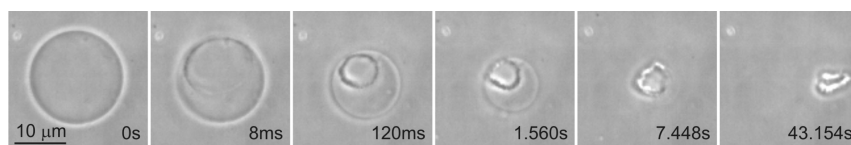
Figure 3. Microscopy images obtained with fast camera recordings under phase contrast observation of a vesicle (DOPC/DOPG, 90/10) upon the addition of 10 μL of 0.100 mg/mL chitosan solution. The first snapshot was taken approximately 15 min after adding the chitosan solution.

The data for the second examined concentration of chitosan in the reverse-phase vesicles, 13.5 monomers for every 100 DOPC, show that the increase in adsorbed polymer further raises the bending rigidity of the vesicles. Thus, the entropic membrane fluctuations must be additionally constrained by the increased amount of adsorbed chitosan chains. For the highest concentration of chitosan, 27.1 monomers for every 100 DOPC, it was no longer possible to reproducibly determine the bending rigidity since it was difficult to locate flickering vesicles in the sample. The vesicles appeared tense. Even osmotic deflation of the vesicles achieved either by leaving the observation cell open for about one hour to allow for evaporation or by adding hypertonic solution did not appear to lower the membrane tension. In these cases, we could observe the formation of outward tubular protrusions of the vesicles coupled with slow vesicle size decrease during the osmotic deflation.

We can only speculate about the reason for irreproducible results in the case of high surface concentration of chitosan in the reverse-phase vesicles. One plausible explanation could be that the bending rigidity of these membranes is higher than what the method can access. Another possibility is that the membrane exhibits spontaneous curvature due to asymmetric distribution of the polymer across the bilayer, as we will discuss later (this effect is even more pronounced for the case of the DOPC/DOPG 90/10 vesicles incubated with chitosan, which adsorbs on the external leaflet of the membrane). Evidence for the asymmetry could be the observed outward protrusions on many vesicles indicating the presence of positive spontaneous curvature of the membrane. Spontaneous curvature generates tension,[44,45] which might be the reason why the vesicles become unsuitable for fluctuation analysis.

The increase of bending rigidity due to the presence of chitosan on the membrane of reverse-phase vesicles is an important result, which corroborates previous reports showing alteration of the physical characteristics of liposomal membranes such as the decrease in bilayer repeat distances[20] and the increase in the thermal stability.[19]

Finally, we discuss the mechanical properties of the vesicles incubated with chitosan post formation. The bending rigidity of incubated DOPC vesicles exhibits an even larger increment (Table 1) compared to that observed for the reverse-phase vesicles. This is a direct evidence for the suppression of membrane undulations upon the adsorption of the polysaccharide on the membrane. However, the data is relatively scattered (see the large standard deviation in Table 1 for the vesicles incubated with chitosan), which we attribute to the fact that the incubation protocol does not ensure homogeneous distribution of chitosan among the vesicles as already demonstrated in Figure 2. Obviously, the mixing conditions are not ideal for optimal distribution of the polymer over the vesicles. On the contrary, in the reverse-phase method, the distribution and interaction of chitosan with the phospholipids

is optimized already in the reverse-phase emulsion, prepared before electroformation.[24]

As mentioned above, DOPC/DOPG 90/10 vesicles incubated in chitosan solutions were unstable. One hour of incubation in a vial resulted in the appearance of small aggregated structures with unclear morphology. Only a scarce amount of giant defect-free vesicles could be found. We could measure the bending rigidity on few such exceptional vesicles and obtained values in the range between 49×10^{-20} and 60×10^{-20} J. However, we cannot claim that these are representative values.

Note that in all of the above measurements, care was taken to avoid osmotic shock when mixing the vesicle suspension with the chitosan solution, since the osmolarity of the chitosan solution was adjusted to match that of the vesicle suspension using sucrose. In the same manner, to ensure that pH change was not influencing the vesicle stability, chitosan-free buffer solution with matching osmolarity was mixed with vesicle suspensions in a parallel set of samples. The vesicles remained unaltered suggesting that the only factor influencing the vesicle stability must be the presence of chitosan. Indeed, changes in the bending rigidity of the vesicles caused by pH changes[46] are not expected in our system because the surface charge of the vesicles was also not observed to alter as a function of pH.[30]

3.3. Pore Formation in Incubated DOPC/DOPG 90/10 Vesicles and Adhesion. To understand the mechanism of destabilization of DOPC/DOPG 90/10 vesicles by chitosan, we attempted to directly observe the vesicles upon mixing with the polysaccharide. Similar studies on giant vesicles addressing the disruption of membranes induced by antimicrobial peptides have been reported previously,[47−50] but have not been applied to chitosan. An aliquot of 50 μL suspension of electroformed vesicles and 150 μL of isotonic glucose solution were placed in an observation chamber under the microscope. The final lipid concentration, assuming no losses, was estimated to be 2.12×10^{-3} mM. After a few minutes allowing for the vesicles to sediment to the bottom slide, a certain amount of chitosan solution (5, 10, 20, 30, or 40 μL) at a concentration of 0.100 mg/mL was carefully added by means of a micropipet and the chamber was immediately closed.

After several minutes, we could directly observe the vesicle restructuring and destabilization resulting from the adsorption of chitosan. Surprisingly, under phase contrast we detected the formation of microscopic pores (larger than 10 μm in diameter) which opened within less than 8 ms followed by vesicle collapse and slower restructuring into some kind of microaggregate or "microgel"; see Figure 3. In some occasions, after the formation of a microscopic pore, the vesicle resealed into a smaller one but continued to lose optical contrast, which is an indication for the presence of submicroscopic pores.

We noticed a correlation between the probability of pore formation and the amount of chitosan added to the observation cell. The higher the amount of chitosan, the faster the vesicles collapsed. With only 5 μL of chitosan solution added into the

observation cell, the vesicles remained unaltered during at least 1 h. Instead with 40 μL, the response was detected after about five minutes. Probably, the larger volumes added allow for faster mixing of the solutions in the observation chamber, but also the higher final concentration of chitosan results in a more pronounced change.

The collapse of the vesicles suggests that the adsorption of the polymer builds up tension in the membrane. Above some critical (lysis) tension the vesicles rupture. Because of the asymmetric distribution of the polymer across the membrane (which might be also inhomogeneous along the vesicle surface), we expect that the polymer adsorption strongly increases the spontaneous curvature of the bilayer. The spontaneous tension associated with this increase[44,45] reaches the lysis tension and the vesicles collapse. Vesicle destabilization based on the effect of spontaneous tension may not necessarily occur with systems based on small vesicles, for example, large unilamellar vesicles (LUVs) as used in ref 30, in the same polymer-to-lipid concentration ranges. The LUV membranes exhibit high curvature on their own, and the adsorption of polymer may not always result in strong bending of the bilayer.

Pore formation induced by chitosan has been shown on membranes of Gram negative bacteria, such as *Escherichia coli*, which exhibits overall negative charge on the surface. Chitosan was demonstrated to disrupt the outer membrane of bacteria by interfering on the negatively charged residues of macro-molecules at the cell surface,[26] altering the permeability of the membrane[25] and causing leakage of intracellular compo-nents and cell agglutination.[27] Such characteristics confer to chitosan the potential for a variety of applications, not only biological, but also pharmaceutical, agricultural and nutritional; for reviews, see refs 51 and 52.

Despite the relatively extended literature on chitosan antibacterial activity, the mechanism of cell membrane disruption is still unclear and hence a subject of investigation. The negatively charged phosphate groups in phospholipids may represent one of the molecular targets of chitosan.[18,53] Our objective in the present work is far from identifying the mechanism of cell membrane disruption induced by chitosan. However, the behavior of the negatively charged giant vesicles incubated with chitosan suggests that they represent a very suitable model for studying pore formation, morphology alteration and final disruption and irreversible damage. For example, the dynamics of the pore opening could be employed to reveal the effect of chitosan on the membrane edge tension and pore stabilization.[54] The time course of leakage and vesicle destabilization can be employed to reveal more about the antimicrobial action of chitosan.[48] Phase separation and lipid segregation induced by the adsorption of the polymer[35] may be yet another course to explore.

To conclude the description about the morphological changes induced by chitosan, here we will briefly discuss some observations on the interaction of the composite vesicles with negatively charged surfaces. Such studies are relevant for development of drug delivery systems if one aims to target modified liposomes to specific cell surfaces.[55−57]

Glass exhibits negative surface charge when immersed in aqueous solutions due to the dissociation of silanol groups. Most glass slides applied in our microscopy observations have been precoated with BSA (see Experimental Section) to avoid adhesion and burst of the chitosomes. However, trials with uncoated glass slides have also shown an interesting peculiarity.

Incubated DOPC vesicles were placed in an observation chamber constructed from uncoated glass slides. Upon adsorption to the glass and rupture, vesicle skeleton-like traces could be observed on the glass surface; see Figure 4. The traces
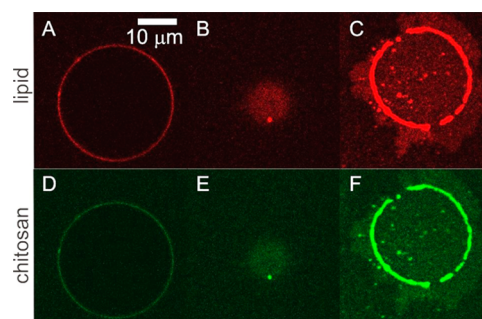
Figure 4. Confocal microscopy images of a giant DOPC vesicle containing fluorescently labeled DPPE-Rhod (red; A−C) and chitosan (green; D−F). The snapshots were taken after incubation of the vesicle with chitosan. (A, D) Equatorial cross sections of the vesicle before rupture. (B, E) Images of the lower pole of the vesicle in close proximity with the glass substrate before rupture. (C, F) Strong fluorescent ring and stains over the glass surface where the vesicle collapsed, suggesting membrane adhesion, rearrangement, and spread-ing over the negatively charged glass surface.

(Figure 4C, F) represented a circular imprint of strong fluorescence of chitosan and labeled lipid, surrounded by an area of weak fluorescence from chitosan-coated membrane adsorbed to the glass. The membrane has adhered and spread over the glass surface (weakly fluorescent areas), but parts of the vesicle have rearranged into a ringlike structure where the membrane might have folded onto itself held together by the externally adsorbed polymer (highly fluorescent regions). The interaction with the glass must be of electrostatic nature, mediated by the positive amino groups of the chitosan monomers and the negative surface charges of the glass.

4. CONCLUDING REMARKS

Using confocal microscopy, we confirm that chitosan is indeed on the membrane for both reverse-phase and incubated vesicles. However, the data also evidence that for the incubated vesicles the distribution of the polymer is highly inhomoge-neous both between vesicles from the same batch (Figure 2) and along the vesicle surface of an individual vesicle (Figure 1). This outcome questions in general the reliability of quantitative data collected on incubated giant vesicles.[34]

The mechanical properties of the decorated membranes were also characterized. Membrane undulations were found to significantly reduce upon incorporation of chitosan. The bending stiffness increases with chitosan concentration denoting physical restrictions imposed to the bilayer as well as electrostatic self-repulsion of the membrane as a consequence of the adsorbed polysaccharide.

Pore formation in giant vesicles (DOPC/DOPG 90/10) is another consequence of chitosan interaction with the negatively charged phospholipids. The vesicles lose optical contrast evidencing exchange between internal and external solutions through the pores, suffer size reduction and final morphology alteration. Such characteristic shows the potential of chitosan in affecting permeability and disrupting negatively charged membranes. After completing the morphological modification of DOPG containing vesicles, chitosan and phospholipids

remain colocalized in the microaggregates, denoting strong and irreversible binding.

For the neutral vesicles, the adhesion of chitosan-covered vesicles on the glass slides shows the capacity of such composite structures to interact with and adhere over negatively charged surfaces. The lifetime of partial adhesion over the surface is still not under control and is beyond the objectives of the present study. However, this behavior shows the potential of these composite vesicles for application as drug delivery systems where the interaction with specific cell membranes is required for the optimization of treatments.

Because of the wide use of chitosan in drug delivery systems, measurements on the mechanical properties of these systems exemplified by carrier vesicles are highly relevant. Namely, it is important to know how stable chitosan-coated membranes are, how easy it is to deform them as the chitosomes travel in the recipient body, and whether they adhere to specific surfaces. Our study unequivocally demonstrates that these questions can be directly answered with studies on giant vesicles as we do here. We emphasize, however, that the different types of preparations of chitosan-coated GUVs result in significant difference in the adsorption behavior.

■ ASSOCIATED CONTENT

ⓈSupporting Information

Table of probed vesicle compositions, confocal microscopy images, and description of the intensity analysis. This material is available free of charge via the Internet at http://pubs.acs.org

■ AUTHOR INFORMATION

Corresponding Authors
*E-mail: Mertins@if.usp.br.
*E-mail: Rumiana.Dimova@mpikg.mpg.de.

Present Address
[†]O.M.: Department of Applied Physics, Institute of Physics, University of Sao Paulo, Rua do Matao, Travessa R 187, 05508-090 Sao Paulo, Brazil.

Notes
The authors declare no competing financial interest.

■ ACKNOWLEDGMENTS

■ REFERENCES

(1) Goethals, E. C.; Elbaz, A.; Lopata, A. L.; Bhargava, S. K.; Bansal, V. Decoupling the Effects of the Size, Wall Thickness, and Porosity of Curcumin-Loaded Chitosan Nanocapsules on Their Anticancer Efficacy: Size Is the Winner. *Langmuir* **2013**, *29* (2), 658–666.

(2) Liu, K. C.; Yeo, Y. Zwitterionic Chitosan-Polyamidoamine Dendrimer Complex Nanoparticles as a pH-Sensitive Drug Carrier. *Mol. Pharmaceutics* **2013**, *10* (5), 1695–1704.

(3) Lima, P. A. L.; Resende, C. X.; de Almeida Soares, G. r. D.; Anselme, K.; Almeida, L. E. Preparation, characterization and biological test of 3D-scaffolds based on chitosan, fibroin and hydroxyapatite for bone tissue engineering. *Mater. Sci. Eng., C* **2013**, *33* (6), 3389–3395.

(4) Prabaharan, M. Prospects of Biosensors Based on Chitosan Matrices. *J. Chitin Chitosan Sci.* **2013**, *1* (1), 2–12.

(5) Bhattarai, N.; Ramay, H. R.; Gunn, J.; Matsen, F. A.; Zhang, M. Q. PEG-Grafted Chitosan As an Injectable Thermosensitive Hydrogel for Sustained Protein Release. *J. Controlled Release* **2005**, *103* (3), 609–624.

(6) Chenite, A.; Chaput, C.; Wang, D.; Combes, C.; Buschmann, M. D.; Hoemann, C. D.; Leroux, J. C.; Atkinson, B. L.; Binette, F.; Selmani, A. Novel Injectable Neutral Solutions of Chitosan Form Biodegradable Gels in Situ. *Biomaterials* **2000**, *21* (21), 2155–2161.

(7) Torrecilla, D.; Lozano, M. V.; Lallana, E.; Neissa, J. I.; Novoa-Carballal, R.; Vidal, A.; Fernandez-Megia, E.; Torres, D.; Riguera, R.; Alonso, M. J.; Dominguez, F. Anti-Tumor Efficacy of Chitosan-g-poly(ethylene glycol) Nanocapsules Containing Docetaxel: Anti-TMEFF-2 Functionalized Nanocapsules vs Non-Functionalized Nanocapsules. *Eur. J. Pharm. Biopharm.* **2013**, *83* (3), 330–337.

(8) Yang, L. R.; Zaharoff, D. A. Role of Chitosan Co-Formulation in Enhancing Interleukin-12 Delivery and Antitumor Activity. *Biomaterials* **2013**, *34* (15), 3828–3836.

(9) Na, J. H.; Lee, S. Y.; Lee, S.; Koo, H.; Min, K. H.; Jeong, S. Y.; Yuk, S. H.; Kim, K.; Kwon, I. C. Effect of the Stability and Deformability of Self-Assembled Glycol Chitosan Nanoparticles on Tumor-Targeting Efficiency. *J. Controlled Release* **2012**, *163* (1), 2–9.

(10) de la Fuente, M.; Ravifia, M.; Paolicelli, P.; Sanchez, A.; Seijo, B. a.; Alonso, M. J. Chitosan-Based Nanostructures: A Delivery Platform for Ocular Therapeutics. *Adv. Drug Delivery Rev.* **2010**, *62* (1), 100–117.

(11) Li, X. F.; Feng, X. Q.; Yang, S.; Fu, G. Q.; Wang, T. P.; Su, Z. X. Chitosan Kills Escherichia coli through Damage to Be of Cell Membrane Mechanism. *Carbohydr. Polym.* **2010**, *79* (3), 493–499.

(12) Gonçalves, M. C. F.; Mertins, O.; Pohlmann, A. R.; Silveira, N. P.; Guterres, S. S. Chitosan Coated Liposomes as an Innovative Nanocarrier for Drugs. *J. Biomed. Nanotechnol.* **2012**, *8* (2), 240–250.

(13) Gordon, S.; Young, K.; Wilson, R.; Rizwan, S.; Kemp, R.; Rades, T.; Hook, S. Chitosan Hydrogels Containing Liposomes and Cubosomes As Particulate Sustained Release Vaccine Delivery Systems. *J. Liposome Res.* **2012**, *22* (3), 193–204.

(14) Lee, J. H.; Oh, H.; Baxa, U.; Raghavan, S. R.; Blumenthal, R. Biopolymer-Connected Liposome Networks as Injectable Biomaterials Capable of Sustained Local Drug Delivery. *Biomacromolecules* **2012**, *13* (10), 3388–3394.

(15) Rescia, V. C.; Ramos, H. R.; Takata, C. S.; de Araujo, P. S.; da Costa, M. H. B. Diphtheria Toxoid Conformation in the Context of Its Nanoencapsulation within Liposomal Particles Sandwiched by Chitosan. *J. Liposome Res.* **2011**, *21* (2), 116–123.

(16) Marón, L. B.; Covas, C. P.; da Silveira, N. P.; Pohlmann, A.; Mertins, O.; Tatsuo, L. N.; Sant'Anna, O. A. B.; Moro, A. M.; Takata, C. S.; de Araujo, P. S.; Bueno da Costa, M. H. LUVs Recovered with Chitosan: A New Preparation for Vaccine Delivery. *J. Liposome Res.* **2007**, *17* (3–4), 155–163.

(17) Mertins, O.; Dimova, R. Binding of Chitosan to Phospholipid Vesicles Studied with Isothermal Titration Calorimetry. *Langmuir* **2011**, *27* (9), 5506–5515.

(18) Mertins, O.; Schneider, P. H.; Pohlmann, A. R.; da Silveira, N. P. Interaction between Phospholipids Bilayer and Chitosan in Liposomes Investigated by P-31 NMR Spectroscopy. *Colloids Surf., B* **2010**, *75* (1), 294–299.

(19) Mertins, O.; Lionzo, M. I. Z.; Micheletto, Y. M. S.; Pohlmann, A. R.; da Silveira, N. P. Chitosan Effect on the Mesophase Behavior of Phosphatidylcholine Supramolecular Systems. *Mater. Sci. Eng., C* **2009**, *29* (2), 463–469.

(20) Mertins, O.; Cardoso, M. B.; Pohlmann, A. R.; da Silveira, N. P. Structural Evaluation of Phospholipidic Nanovesicles Containing Small Amounts of Chitosan. *J. Nanosci. Nanotechnol.* **2006**, *6* (8), 2425–2431.

(21) Dimova, R. Giant Vesicles: A Biomimetic Tool for Membrane Characterization. In *Advances in Planar Lipid Bilayers and Liposomes*; Iglic, A., Ed.; Academic Press: London, 2012; Vol. 16, pp 1–50.

(22) Dimova, R.; Aranda, S.; Bezlyepkina, N.; Nikolov, V.; Riske, K. A.; Lipowsky, R. A Practical Guide to Giant Vesicles. Probing the

Membrane Nanoregime via Optical Microscopy. *J. Phys.: Condens. Matter* **2006**, *18* (28), S1151−S1176.

(23) Quemeneur, F.; Rammal, A.; Rinaudo, M.; Pepin-Donat, B. Large and Giant Vesicles "Decorated" with Chitosan: Effects of pH, Salt or Glucose Stress, and Surface Adhesion. *Biomacromolecules* **2007**, *8* (8), 2512−2519.

(24) Mertins, O.; da Silveira, N. P.; Pohlmann, A. R.; Schroder, A. P.; Marques, C. M. Electroformation of Giant Vesicles from an Inverse Phase Precursor. *Biophys. J.* **2009**, *96* (7), 2719−2726.

(25) Young, D. H.; Kohle, H.; Kauss, H. Effect of Chitosan on Membrane-Permeability of Suspension-Cultured Glycine-Max and Phaseolus-Vulgaris Cells. *Plant Physiol.* **1982**, *70* (5), 1449−1454.

(26) Young, D. H.; Kauss, H. Release of Calcium from Suspension-Cultured Glycine-Max Cells by Chitosan, Other Polycations, and Polyamines in Relation to Effects on Membrane-Permeability. *Plant Physiol.* **1983**, *73* (3), 698−702.

(27) Helander, I. M.; Nurmiaho-Lassila, E. L.; Ahvenainen, R.; Rhoades, J.; Roller, S. Chitosan Disrupts the Barrier Properties of the Outer Membrane of Gram-Negative Bacteria. *Int. J. Food Microbiol.* **2001**, *71* (2−3), 235−244.

(28) Godderz, L. J.; Peak, M. M.; Rodgers, K. K. Analysis of Biological Macromolecular Assemblies Using Static Light Scattering Methods. *Curr. Org. Chem.* **2005**, *9* (9), 899−908.

(29) Qaqish, R. B.; Amiji, M. M. Synthesis of a Fluorescent Chitosan Derivative and Its Application for the Study of Chitosan-Mucin Interactions. *Carbohydr. Polym.* **1999**, *38* (2), 99−107.

(30) Mertins, O.; Dimova, R. Insights on the Interactions of Chitosan with Phospholipid Vesicles. Part I: Effect of Polymer Deionization. *Langmuir* **2013**, DOI: 10.1021/la403218c.

(31) Gracià, R. S.; Bezlyepkina, N.; Knorr, R. L.; Lipowsky, R.; Dimova, R. Effect of Cholesterol on the Rigidity of Saturated and Unsaturated Membranes: Fluctuation and Electrodeformation Analysis of Giant Vesicles. *Soft Matter* **2010**, *6* (7), 1472−1482.

(32) Akashi, K.; Miyata, H.; Itoh, H.; Kinosita, K. Formation of Giant Liposomes Promoted by Divalent Cations: Critical Role of Electrostatic Repulsion. *Biophys. J.* **1998**, *74* (6), 2973−2982.

(33) Quemeneur, F.; Rinaudo, M.; Pepin-Donat, B. Influence of Molecular Weight and pH on Adsorption of Chitosan at the Surface of Large and Giant Vesicles. *Biomacromolecules* **2008**, *9* (1), 396−402.

(34) Quemeneur, F.; Rinaudo, M.; Maret, G.; Pepin-Donat, B. Decoration of Lipid Vesicles by Polyelectrolytes: Mechanism and Structure. *Soft Matter* **2010**, *6* (18), 4471−4481.

(35) Pataraia, S.; Liu, Y.; Lipowsky, R.; Dimova, R., Effect of Cytochrome *c* on the Phase Behavior of Charged Multicomponent Lipid Membranes. Submitted.

(36) Pan, J.; Tristram-Nagle, S.; Kucerka, N.; Nagle, J. F. Temperature Dependence of Structure, Bending Rigidity, And Bilayer Interactions of Dioleoylphosphatidylcholine Bilayers. *Biophys. J.* **2008**, *94* (1), 117−124.

(37) Rawicz, W.; Olbrich, K. C.; McIntosh, T.; Needham, D.; Evans, E. Effect of Chain Length and Unsaturation on Elasticity of Lipid Bilayers. *Biophys. J.* **2000**, *79* (1), 328−339.

(38) Winterhalter, M.; Helfrich, W. Bending Elasticity of Electrically Charged Bilayers - Coupled Monolayers, Neutral Surfaces, And Balancing Stresses. *J. Phys. Chem.* **1992**, *96* (1), 327−330.

(39) Mitchell, D. J.; Ninham, B. W. Curvature Elasticity of Charged Membranes. *Langmuir* **1989**, *5* (4), 1121−1123.

(40) Pincus, P.; Joanny, J. F.; Andelman, D. Electrostatic Interactions, Curvature Elasticity, and Steric Repulsion in Multimembrane Systems. *Europhys. Lett.* **1990**, *11* (8), 763−768.

(41) Song, J.; Waugh, R. E. Bilayer-Membrane Bending Stiffness by Tether Formation from Mixed Pc-Ps Lipid Vesicles. *J. Biomech. Eng.* **1990**, *112* (3), 235−240.

(42) Vitkova, V.; Cenova, J.; Finogenova, O.; Mitov, M. D.; Ermakov, Y.; Bivas, I. Surface Charge Effect on the Bending Elasticity of Lipid Bilayers. *C. R. Acad. Bulg. Sci.* **2004**, *57* (11), 25.

(43) Rowat, A. C.; Hansen, P. L.; Ipsen, J. H. Experimental Evidence of the Electrostatic Contribution to Membrane Bending Rigidity. *Europhys. Lett.* **2004**, *67* (1), 144−149.

(44) Li, Y.; Lipowsky, R.; Dimova, R. Membrane Nanotubes Induced by Aqueous Phase Separation and Stabilized by Spontaneous Curvature. *Proc. Natl. Acad. Sci. U.S.A.* **2011**, *108* (12), 4731−4736.

(45) Lipowsky, R. Spontaneous Tubulation of Membranes and Vesicles Reveals Membrane Tension Generated by Spontaneous Curvature. *Faraday Discuss.* **2013**, *161*, 305−331.

(46) Zhou, Y.; Raphael, R. M. Solution pH Alters Mechanical and Electrical Properties of Phosphatidylcholine Membranes: Relation between Interfacial Electrostatics, Intramembrane Potential, and Bending Elasticity. *Biophys. J.* **2007**, *92* (7), 2451−2462.

(47) Tamba, Y.; Yamazaki, M. Single Giant Unilamellar Vesicle Method Reveals Effect of Antimicrobial Peptide Magainin 2 on Membrane Permeability. *Biochemistry* **2005**, *44* (48), 15823−15833.

(48) Ambroggio, E. E.; Separovic, F.; Bowie, J. H.; Fidelio, G. D.; Bagatolli, L. A. Direct Visualization of Membrane Leakage Induced by the Antibiotic Peptides: Maculatin, Citropin, and Aurein. *Biophys. J.* **2005**, *89* (3), 1874−1881.

(49) Tamba, Y.; Ohba, S.; Kubota, M.; Yoshioka, H.; Yoshioka, H.; Yamazaki, M. Single GUV Method Reveals Interaction of Tea Catechin (−)-Epigallocatechin Gallate with Lipid Membranes. *Biophys. J.* **2007**, *92* (9), 3178−3194.

(50) Lee, M. T.; Hung, W. C.; Chen, F. Y.; Huang, H. W. Mechanism and Kinetics of Pore Formation in Membranes by Water-Soluble Amphipathic Peptides. *Proc. Natl. Acad. Sci. U.S.A.* **2008**, *105* (13), 5087−5092.

(51) Shahidi, F.; Arachchi, J. K. V.; Jeon, Y. J. Food Applications of Chitin and Chitosans. *Trends Food Sci. Technol.* **1999**, *10* (2), 37−51.

(52) Rinaudo, M. Chitin and Chitosan: Properties and Applications. *Prog. Polym. Sci.* **2006**, *31* (7), 603−632.

(53) Xing, K.; Chen, X. G.; Liu, C. S.; Cha, D. S.; Park, H. J. Oleoyl-Chitosan Nanoparticles Inhibits *Escherichia coli* and *Staphylococcus aureus* by Damaging the Cell Membrane and Putative Binding to Extracellular or Intracellular Targets. *Int. J. Food Microbiol.* **2009**, *132* (2−3), 127−133.

(54) Portet, T.; Dimova, R. A New Method for Measuring Edge Tensions and Stability of Lipid Bilayers: Effect of Membrane Composition. *Biophys. J.* **2010**, *99* (10), 3264−3273.

(55) Takeuchi, H.; Yamamoto, H.; Niwa, T.; Hino, T.; Kawashima, Y. Enteral Absorption of Insulin in Rats from Mucoadhesive Chitosan-Coated Liposomes. *Pharm. Res.* **1996**, *13* (6), 896−901.

(56) Takeuchi, H.; Matsui, Y.; Sugihara, H.; Yamamoto, H.; Kawashima, Y. Effectiveness of Submicron-Sized, Chitosan-Coated Liposomes in Oral Administration of Peptide Drugs. *Int. J. Pharm.* **2005**, *303* (1−2), 160−170.

(57) Sugihara, H.; Yamamoto, H.; Kawashima, Y.; Takeuchi, H. Effectiveness of Submicronized Chitosan-Coated Liposomes in Oral Absorption of Indomethacin. *J. Liposome Res.* **2012**, *22* (1), 72−79.